NMR IN BIOMEDICINE
NMR Biomed. 2003;**16**:137–143
Published online in Wiley InterScience (www.interscience.wiley.com). DOI:10.1002/nbm.819

Improved spatial localization based on flow-moment-nulled and intra-voxel incoherent motion-weighted fMRI

Allen W. Song* and Tianlu Li

Brain Imaging and Analysis Center, Duke University, Durham, NC 27710, USA

Received 9 January 2003; Revised 28 February 2003; Accepted 24 March 2003

ABSTRACT: Functional MRI signal based on the blood oxygenation level-dependent contrast can reveal brain vascular activities secondary to neuronal activation. It could, however, arise from vascular compartments of all sizes, and in particular, be largely influenced by contributions of large vein origins that are distant from the neuronal activities. Alternative contrasts can be generated based on the cerebral blood flow or volume changes that would provide complementary information to help achieve more accurate localization to the small vessel origins. Recent reports also indicated that apparent diffusion coefficient-based contrast using intravoxel incoherent motion (IVIM) weighting could be used to efficiently detect synchronized signal changes with the functional activities. It was found that this contrast has significant arterial contribution where flow changes are more dominant. In this study, a refined approach was proposed that incorporated the flow-moment-nulling (FMN) strategy to study signal changes from the brain activation. The results were then compared with those from conventional IVIM- and BOLD-weighted acquisitions. It was shown that the activated region using the new acquisition strategy had smaller spatial extent, which was contained within the activated areas from the other two methods. Based on the known characteristics of the conventional IVIM and BOLD contrasts, it was inferred that the FMN–IVIM acquisition had improved selective sensitivity towards smaller vessels where volume changes were prevalent. Therefore, such an acquisition method may provide more specific spatial localization closely coupled to the true neuronal activities.

KEYWORDS: fMRI; BOLD; ADC; flow moment; IVIM; diffusion weighting

INTRODUCTION

The field of functional neuroimaging research has seen rapid progress in the past decade, driven by the explosive growth of functional magnetic resonance imaging (fMRI).[1–6] The fMRI signal, based on the blood oxygenation level dependent (BOLD) contrast,[7] has proven to be a robust secondary effect as a result of neuronal activity. However, because of its sensitivity to a wide range of vasculature as the blood oxygenation level changes are the results of changing cerebral blood flow (CBF) or volume (CBV) within these networks, the signal localization ability of the BOLD technique to the true neuronal activities is compromised.[8–10] Alternative methods that can detect changes in CBF[11–13] and CBV[14–16] were adopted to provide complementary information that can lead to more detailed understanding on the response of the brain vasculature to neuronal activation and, in turn, to better localization to the small vessel networks that are closely coupled to the true neuronal activities.

Because of the mutual influences among the blood oxygenation level, CBF and CBV changes are not yet fully understood, investigations that integrated multiple contrasts in one experiment have been carried out to understand their coupling mechanism. Methods that allowed simultaneous non-invasive assessment of the BOLD and CBF changes[17–26] have been developed and it was suggested that arterial spin-labeled CBF imaging may lead to better localization to the smaller vessel networks.[27] The application of CBV contrast in fMRI were used less frequently in humans as most of the traditional techniques require exogenous contrast agents which are not easily applicable in normal human studies.

Recent reports[28–30] demonstrated that the apparent diffusion coefficient (ADC) contrast based on the intravoxel incoherent motion[31,32] (IVIM) model can also be used to detect task-induced signal changes. Similar to the conventional CBF changes observed by ASL methodology with resultant perfusion maps reflecting

**Correspondence to:* A. W. Song, Brain Imaging and Analysis Center, Box 3918, Duke University Medical Center, Durham, NC 27710, USA.
Email: allen.song@duke.edu

Abbreviations used: ADC, apparent diffusion coefficient; BOLD, blood oxygen level dependent; CBF, cerebral blood flow; CBV, cerebral blood volume; FMN, flow-moment-nulled; IVIM, intravoxel incoherent motions.

the changes of both the blood flow velocity v and volume fraction f, the signal changes based on the ADC contrast were also dependent upon these two factors. However, they may have a higher temporal resolution compared with those from ASL methods since the ADC technique does not require a delay time to allow tagged blood to enter the imaging slice. It was shown that ADC contrast mainly originated from arterial and possibly capillary networks,[33] but it remained difficult to break down the components of the ADC changes and correlate them to the exact vascular compartments. Subsequently, experiments using simultaneous BOLD and ADC contrasts were carried out to jointly assess the areas with flow and oxygenation level changes.[30] Based on the spatial overlaps and discrepancies between the BOLD- and ADC-activated areas, several compartments were delineated that showed prevailing sensitivity to different vascular pools, including smaller vessels such as capillaries.

It would be desirable, however, to be able to achieve small vessel localization using a single contrast. The afore-mentioned ADC contrast contains contributions from arteries, arterioles and capillaries, within which both the velocity and volume changes can be present. One possible approach would be to separate the smaller arteriole and capillary contributions from the arterial contributions. Studies using optical imaging have shown that task-induced blood volume changes occurred much more significantly at the level of arterioles and capillaries than at the level of arteries.[34–36] Thus, a refined approach that is capable of generating ADC contrast independent of the velocity changes could be used to directly detect CBV changes in the smaller vessels. Specifically, we describe in this report a new technique, which incorporates a flow-moment-nulling (FMN) strategy into the ADC contrast using the IVIM weighting method to largely remove the dependency on velocity changes. Its performance was compared with those from the conventional IVIM- and BOLD-weighted techniques. It is worth noting that the draining veins also experience volume changes, owing to increased blood flow upstream. However, appropriate parameter settings (e.g. a small amount of initial diffusion weighting) can be used to first suppress the large vessel effect.

METHODS

Previous reports using a conventional IVIM weighting have demonstrated that the ADC contrast can be used to detect task-induced signal changes.[28,29] In a very recent report,[30] it was shown that the signal attenuation factor F of a specific IVIM weighting strategy can be approximated by $F = |f \cdot J_o(cv) + (1-f)\cdot e^{-bD_{brain}}|$, where f is the volume fraction of the vasculature, c the flow moment coefficient of the gradient waveform used for the IVIM weighting, v the blood velocity to the first order, J_o the Bessel function, b the inherent diffusion weighting factor, and D_{brain} the diffusion coefficient of the brain tissue. This equation was derived from a simplified two-compartment model (vasculature and parenchyma) for the human brain, in which other proton pools such as the CSF were not considered, even though it would contribute to the resting brain ADC. Nevertheless, it can easily be seen that the functional signal using this method is dependent upon both blood velocity and volume changes.

Flow moment manipulation strategies are often used to image different vasculature based on their velocity differences. In this study we propose to incorporate the FMN strategy into IVIM weighting to study the vascular contribution to the functional signal that is independent of velocity changes. With the flow moment nulled ($c = 0$), the signal attenuation factor F can be approximated as $F = |f \cdot e^{-bD_{static\_blood}} + (1-f) \cdot e^{-bD_{brain}}|$, where D_{static_blood} is the ADC of static blood, and D_{brain} the ADC of brain tissue. As a result, the FMN strategy generated signal changes mostly dependent upon the blood volume fraction (f) changes. If we denote D as the ADC of the measured signal, then

$$e^{-bD} = |f \cdot e^{-bD_{static\_blood}} + (1-f) \cdot e^{-bD_{brain}}| \quad (1)$$

Note that the exponential fitting procedures were carried out separately within the steady states of resting and active conditions. Thus, changes in relaxation effects and proton density from the resting to the active condition will not affect the derivation of individual D within the two states. These factors are therefore not reflected in eqn (1). For very small b-factors ($bD \ll 1$), which is true for our experiments under flow moment nulling, eqn. (1) can be simplified to

$$D \approx D_{brain} + f(D_{static\_blood} - D_{brain}) \quad (2)$$

Since proton pools such as the CSF would also contribute to the ADC value of the brain in this model, and their volume fraction remains difficult to determine within the scope of this paper, one could not use eqn (2) to obtain an accurate estimate of the absolute blood volume fraction. However, it can be derived, by taking the difference of the D at active and resting conditions, that $\Delta D \propto \Delta f$. This relationship indicates that the changes of ADC values under flow moment nulling can reflect the changes in blood volume. Of course, the above derivation was based on the assumption that D_{static_blood} and D_{brain} are constants. While there was no evidence that D_{static_blood} changed during brain activation, a recent report[37] suggested that D_{brain} would experience a small reduction potentially due to cell swelling during brain activation. This reduction in ADC value, however, would not reverse the positive correlation between ΔD and Δf, as that would require the blood volume fraction f to increase even further to result in an increase of D.

Based on the above discussion, a method that enabled

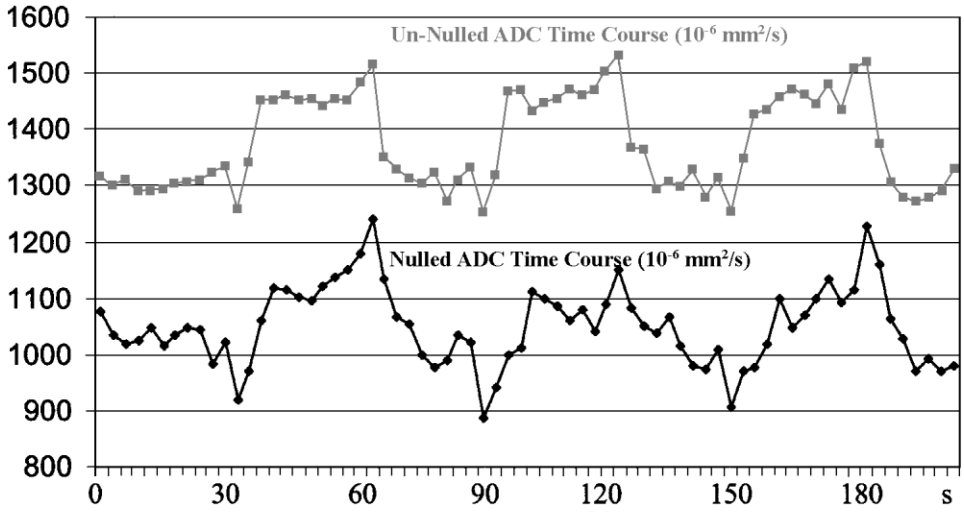

Figure 1. Averaged time courses for both ADC contrasts across all six subjects: the time course from the FMN acquisition is shown in black, and that from the conventional un-nulled acquisition is shown in gray; the unit for the time course is 10^{-6} mm^2/s

FMN acquisition was implemented. This method applied the often-used multi-lobe motion sensitizing gradient to achieve both the IVIM weighting and flow moment nulling.[38] Parallel experiments using conventional IVIM weighting without flow moment nulling but with the same weighting strength and duration were also carried out to acquire time-course images within the same study. The spatial locations and activation magnitude of the activated areas using the FMN–IVIM acquisition were compared with those obtained with the conventional IVIM- weighted acquisition. In addition, they were also compared with those obtained from the intrinsically acquired BOLD contrast.

Functional neuronal activity was generated in the visual cortex using a simple flashing checkerboard delivered through an XGA goggle system (Resonance Technology, Northridge, CA, USA). The stimulus was on for three periods, each lasting 30 s and separated by 30 s blank screen. During the 'on' period, the checkerboard was flashing at a 5 Hz rate. The subjects were instructed to fixate on the crosshair in the center of the visual field during the scan and to passively view the visual stimuli.

To allow intrinsic acquisition of BOLD contrast for comparison, gradient-echo spiral functional images were taken within the visual cortex parallel to the Calcarine fissure. Each volume contained four 5 mm-thick oblique-axial slices of a 64×64 matrix at FOV of 24 cm. A repetition time (*TR*) of 1 s and echo time (*TE*) of 50 ms were used. To minimize the inflow contrast, the flip angle was set at 30° to avoid saturating the imaging plane. Three *b*-factors for diffusion/IVIM weighting with flow moment nulled were 2, 37 and 72 s/mm^2, and those for conventional IVIM weighting (with in-plane flow sensitivity of 0.76 rad s/mm) were 2, 116 and 230 s/mm^2. The amplitude and diffusion weighting time for both schemes were kept the same, and because of their different weighting efficiency, the *b*-factor range was different. Thus, the maximum *b*-factor for the FMN isotropic weighing method was smaller than that for the conventional isotropic weighting method. However, both *b*-factor ranges adequately sample the section of the bi-exponential decay curve (between the MR signal and *b*-factors) most sensitive to the intravascular signal changes (typically 0–200 s/mm^2),[28,29] thus the resultant ADC values via an exponential fitting algorithm for both *b*-factor ranges would yield accurate representation of the mobility changes of the intravascular component. The slow component (i.e. the parenchyma) of this bi-exponential decay would not, in principle, change mobility during brain activation, and thus, it would not affect the activation pattern using either the FMN or conventional ADC contrasts. The small initial *b*-factor was important in suppressing signals from large vessels with large ADCs, which helped the ADC contrast to focus on the smaller vessels since this small *b*-factor was used to acquire the baseline signal for the exponential fitting procedure. The three *b*-factors for both weighting strategies were cyclically ramped, with each cycle lasting 3 s given the 1 s *TR*. A total of 70 such cycles (thus 210 volumes) were acquired for each run, generating 70 dynamic points for the ADC time course. Four runs were acquired for each condition (nulled and un-nulled IVIM weighting) within each subject, which were then averaged together to gain statistical power. To serve as anatomical references, a set of T_1-weighted high-resolution co-planar images was also acquired. An exponential fitting algorithm, according to the signal equation under diffusion weighting ($F = e^{-bD}$), was applied to the three signal values in each cycle of the averaged time courses for every voxel, yielding an estimated composite ADC for each voxel at each cycle. This procedure provided a dynamic time course of the ADCs from the resting state

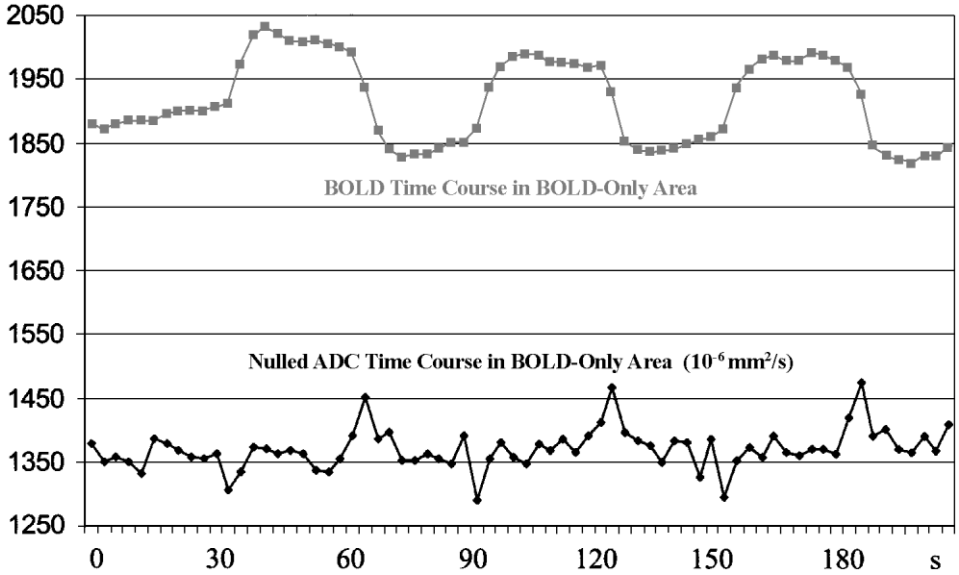

Figure 2. The BOLD time course (shown in gray) and ADC time course (shown in black) within the BOLD-only areas averaged across all six subjects. The lack of ADC activation in the BOLD-only regions is not due to statistical thresholding effect, confirmed by the ADC time course. The unit for BOLD time course is arbitrary, and the unit for ADC time course is 10^{-6} mm^2/s

to activation. A multiple regression algorithm containing the activation paradigm and linear drift as regressors was used to delineate statistically significant areas while effectively detrending any linear drifts in the time course. The same statistical analysis was carried out in the inherently acquired BOLD time courses, which were obtained by gathering the first point of each cycle, to determine activated areas of BOLD contrast. The activation (both the areas and time courses within them) using FMN–IVIM acquisition was compared with those obtained with conventional IVIM- and BOLD-weighted acquisitions.

All images were acquired in the form of raw data (i.e. data before Fourier transformation), which were transported to an SGI Octane workstation (Mountain View, CA, USA) for off-line reconstruction. Six healthy volunteers (mean age 21 years) gave their written consent approved by the Institutional Review Board of Duke University Medical Center to participate in the experiment. The study was performed on a General Electric 4 T whole-body MRI scanner (Milwaukee, WI, USA) running on the LX platform.

RESULTS AND DISCUSSION

The activated areas, using the FMN–IVIM, conventional IVIM-, and BOLD-weighted acquisitions, were determined by statistical significances calculated from the respective time courses of the dynamic ADCs. The z-score maps, with a threshold of $z > 3.0$, were overlaid on high resolution T_1-weighted images to illustrate these areas. The comparisons of the activated areas and averaged time courses were made between the FMN- and conventional IVIM-weighted acquisitions. In addition, the activation patterns of both IVIM-weighted acquisitions were compared to that of BOLD contrast.

Plate 1(a) shows activation maps from a representative subject containing three slices through the calcarine fissure indicating the responses from the primary visual cortex, using the two IVIM-weighted acquisitions. The significant activation based on the ADC changes under FMN–IVIM weighting is shown in translucent red, and the activation based on the ADC changes under conventional IVIM weighting is shown in translucent blue. Significant spatial overlap can be seen between these two contrasts, with the activation from FMN acquisition showing a more reduced spatial extent than and contained mostly within that of the conventional IVIM acquisition. This smaller spatial extent is the result of the reduced sensitivity to the velocity changes in the FMN ADC contrast. Plate 1(b) and (c) shows the activated areas (in translucent red) using the FMN acquisition and conventional IVIM acquisition overlaid on the activated area (in translucent blue) using the BOLD contrast, respectively. It was shown that FMN activations had much smaller spatial extent than, and were well within, the areas identified using the BOLD contrast. In comparison, the activation using conventional IVIM weighting showed more significant spatial discrepancy with that of the BOLD contrast.

Across subjects, our combined spatial assessment revealed that, using the same threshold for statistical significance; BOLD activation had the largest spatial

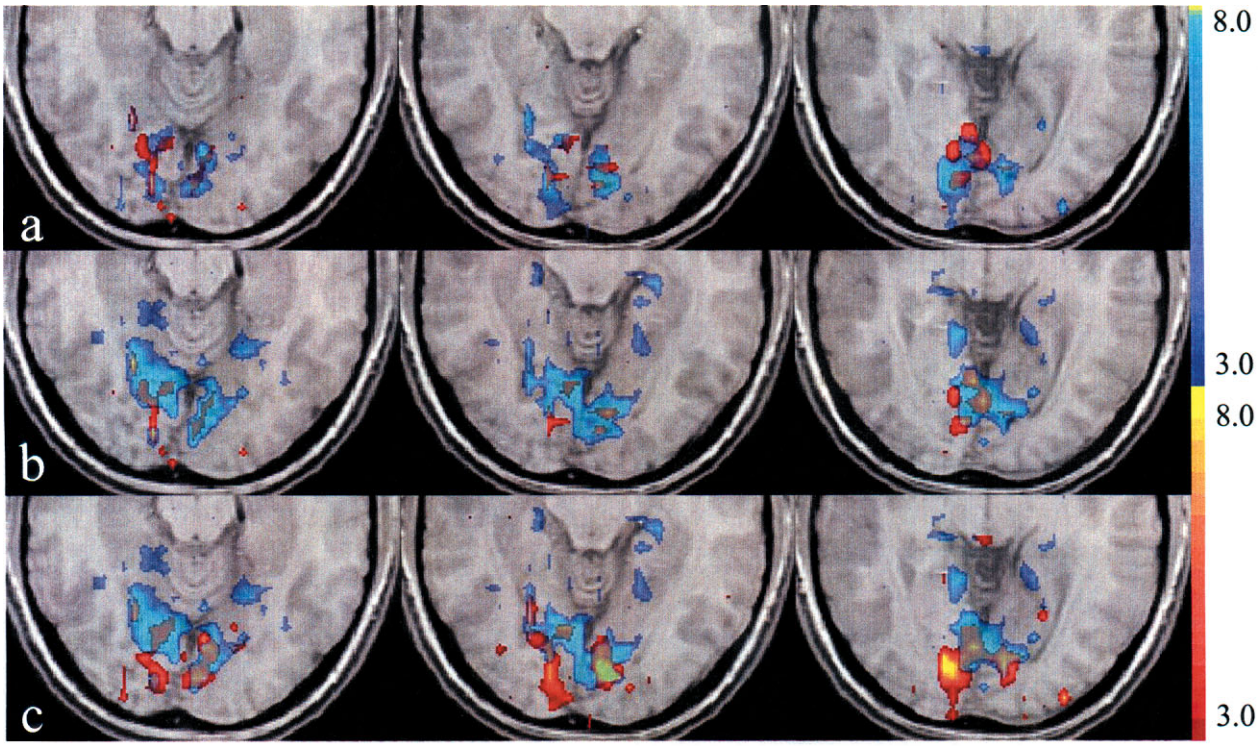

Plate 1. (a) Activation maps ($3.0 < z < 8.0$) based on the ADC contrast using both the FMN and conventional (un-nulled) IVIM acquisition from one representative subject. The activation from the nulled weighting scheme is shown in translucent red, and that from the un-nulled weighting scheme is shown in translucent blue. Significant FMN-ADC activation occurs within the activated areas using conventional ADC contrast. (b) Activation maps ($3.0 < z < 8.0$) based on the FMN-ADC (in translucent red) and BOLD contrast (in translucent blue) from the same subject. Similar to the results seen in (a), most of the FMN–ADC activation occurs within the BOLD activation. (c) Activation maps ($3.0 < z < 8.0$) based on the conventional ADC (in translucent red) and BOLD contrast (in translucent blue) from the same subject. Note the significant spatial discrepancy along with the overlap

extent, while conventional ADC contrast using IVIM weighting had intermediate spatial extent (73.4% of that of BOLD), and the FMN-ADC activation yielded the smallest extent (25.8% of that of BOLD). The overlap between the FMN-ADC and conventional ADC contrasts accounted for 62.3% (majority) of the total activation using FMN-ADC contrast, and 21.9% of the total activation using conventional ADC contrast. The overlap between the FMN-ADC and BOLD contrasts accounted for 71.0% (the majority) of the total activation using FMN-ADC contrast, and 18.4% of the total activation using BOLD contrast. The overlap between the conventional ADC and BOLD contrasts accounted for 41.3% of the total activation using conventional ADC contrast, and 30.3% of the total activation using BOLD contrast. These measures confirmed the qualitative findings in Plate. 1.

In addition to the spatial assessment, the time courses were also averaged within the commonly activated areas between the two IVIM weighting conditions across all subjects. Fig. 1 shows the respective time courses for both conditions. From the averaged ADC time course, it was estimated that, for FMN acquisition, there was an average change of $8.8 \pm 2.6\%$. The magnitude of this ADC change is smaller than that using the conventional IVIM weighting method ($\sim 11.1 \pm 1.2\%$) derived from the averaged time course. The mean ADC values from the FMN acquisition also showed a 29.5% reduction compared with those obtained from the conventional IVIM method. Both observations were as expected due to the removal of the velocity dependence in the FMN acquisition. It is also worth noting that the time courses of the ADC showed a brief decrease at the onset of the visual stimulation and a brief increase at the offset of the visual stimulation. This was because the transient ascending phase or the descending phase of the BOLD signal artificially suppressed or elevated the resultant ADC values, since the ADC values were obtained by exponentially fitting every three time points. Thus, these artificial spikes were markers for the onset and the offset of the BOLD signal. However, since a block design was used in our experiments, all these transition points were excluded from the statistical analysis. That is, only the time points during steady states were fit for ADC values and used for statistical analysis. Within individually activated areas using the two IVIM methods, the BOLD signal was also averaged across subjects. Larger BOLD activation of 6.9% within the activated areas using the flow-nulled ADC contrast was seen, as opposed to 5.6% for the BOLD activation within the activated areas using the un-nulled ADC contrast. The reduced BOLD activation could be due to averaging effects within a larger activated area using the un-nulled ADC contrast, within which there would be more upstream arterial contributions that experience smaller BOLD signal changes.

There were concerns that the reduced spatial extent may simply be due to the thresholding effect at different statistical significance. For example, since the BOLD activated areas appeared to have a much larger spatial extent, there were significant areas which showed only the BOLD, but not the ADC activities. We thereby reduced statistical thresholds for FMN-ADC contrast to assess their influence on the spatial extent, although such operation resulted in more extraneous activation rather than an increase in spatial extent. To further illustrate such a finding, the BOLD-only regions were used as a mask to average the time courses for both the BOLD and ADC images. The resultant time courses are shown in Fig. 2. The ADC time course confirmed that it showed no detectable activation, however it did show the typical spikes during the onset and offset of the BOLD signal.

Recent reports also suggested that the ADC changes may arise from the interaction between the background gradients and diffusion weighting gradients. Studies using diffusion-weighted spin-echo imaging sequences from Zhong *et al.*[39] and Does *et al.*[40] indicated that background gradients near vessels caused by the susceptibility differences could influence the estimation of ADC, when these background gradients have odd symmetry with the diffusion weighting gradients to offset the effect of diffusion weighting. However, such offsetting effect can only be seen in spin-echo type sequences, since the diffusion weighting gradients, similar to the background gradients, do not change polarity over time. For the gradient-echo sequence used in our report, the diffusion weighting gradients were time varying and did change polarity over time, whereas the background gradients were relatively constant and did not change polarity. As a result, the background gradients cannot be of odd symmetry with diffusion weighting gradients in gradient-echo sequences, and therefore did not influence the ADC estimation as they would have in diffusion-weighted spin-echo sequences.

In summary, the activation using the FMN-IVIM weighting technique identified overlapping areas between the activated regions using conventional IVIM- and BOLD-weighted acquisitions. Since the conventional IVIM method mostly detects signal changes arising from the arteries, arterioles and capillaries, and BOLD activation is sensitive to the veins, venules and capillaries, the overlap between these two contrasts suggests its selective sensitivity to the smaller vessel networks,[30] which are more closely coupled to the true neuronal activities. Thus, the FMN-IVIM acquisition would have a selective sensitivity towards smaller vessel networks (e.g. arterioles and capillaries), where the task-induced volume changes are significant.[34–36]

CONCLUSIONS

A new functional imaging method was demonstrated in which IVIM weighting was used in conjunction with FMN strategies to localize functional signal synchronized to brain activation. Theoretical assessment found that this

new contrast could be predominantly dependent on CBV changes, and experimental evaluation and comparison of the performance of this new method with those of the conventional IVIM- and BOLD-weighted acquisitions suggested that it could have a selective sensitivity to the smaller vascular networks. It is thus anticipated that this new acquisition strategy may be used to efficiently and effectively achieve more specific co-localization of the neuronal activities.

Acknowledgements

This work was supported by grants from the National Science Foundation (BES 0092672) and the National Institutes of Health (NS 41328). The authors thank Dr Gregory McCarthy and Mr Charles Michelich for providing us with handy Matlab® routines.

REFERENCES

1. Belliveau JW, Kennedy DN, McKinstry RC, Buchbinder BR, Weisskoff RM, Cohen MS, Vevea JM, Brady TJ, Rosen BR. Functional mapping of the human visual cortex by magnetic resonance imaging. *Science* 1991; **254**: 716–719.
2. Kwong KK, Belliveau JW, Chesler DA, Goldberg IE, Weisskoff RM, Poncelet BP, Kennedy DN, Hoppel BE, Cohen MS, Turner R, Cheng HM, Brady TJ, Rosen BR. Dynamic magnetic resonance imaging of human brain activity during primary sensory stimulation. *Proc. Natl Acad. Sci. USA* 1992; **89**: 5675–5679.
3. Bandettini PA, Wong EC, Hinks RS, Tikofsky RS, Hyde JS. Time course EPI of human brain function during task activation. *Magn. Reson. Med.* 1992; **25**: 390–397.
4. Ogawa S, Tank DW, Menon R, Ellerman JM, Kim SG, Merkle H, Ugurbil K. Intrinsic signal change accompanying sensory stimulation: functional brain mapping with magnetic resonance imaging. *Proc. Natl Acad. Sci. USA* 1992; **89**: 5951–5955.
5. Menon R, Ogawa S, Tank DW, Ugurbil K. 4 Tesla gradient recalled echo characteristics of photic stimulation-induced signal changes in the human primary visual cortex. *Magn. Reson. Med.* 1993; **30**: 380–386.
6. Turner R, Jezzard P, Wen H, Kwong KK, LeBihan D, Zeffiro T, Balaban RS. Functional mapping of the human visual cortex at 4 and 1.5 Tesla using deoxygenated contrast EPI. *Magn. Reson. Med.* 1993; **29**: 277–279.
7. Ogawa S, Menon RS, Tank DW, Kim SG, Merkle H, Ellerman JM, Ugurbil K. Functional brain mapping by blood oxygenation level dependent contrast magnetic resonance imaging. *Biophys. J.* 1993; **64**: 803–812.
8. Song AW, Wong EC, Tan SG, Hyde JS. Diffusion weighted fMRI at 1.5 T. *Magn. Reson. Med.* 1996; **35**: 155–158.
9. Boxerman JL, Bandettini PA, Kwong KK, Baker JR, Davis TL, Rosen BR, Weisskoff RM. The intravascular contribution to fMRI signal change: monte carlo modeling and diffusion weighted studies *in vivo*. *Magn. Reson. Med.* 1995; **34**: 4–10.
10. Jezzard P, Song AW. Technical foundations and pitfalls of clinical fMRI. *NeuroImage*, 1996; **4**(3): S63–S75.
11. Detre JA, Leigh JS, Williams DS, Koretsky AP. Perfusion imaging. *Magn. Reson. Med.* 1992; **23**: 37–45.
12. Edelman RR, Siewert B, Darby DG, Thangaraj V, Nobre AC, Mesulam MM, Warach S. Qualitative mapping of cerebral blood flow and functional localization with echo-planar MR imaging and signal targeting with alternating radio frequency. *Radiology* 1994; **192**: 513–520.
13. Kim S-G. Quantification of relative cerebral blood flow changes by flow-sensitive alternating inversion recovery (FAIR) technique: application to functional mapping. *Magn. Reson. Med.* 1995; **34**: 293–301.
14. Mandeville JB, Marota JJA, Kosofsky BE, Keltner JR, Weissleder R, Rosen BR, Weisskoff RM. Dynamic functional imaging of relative cerebral blood volume during rat forepaw stimulation. *Magn. Reson. Med.* 1998; **39**: 615–624.
15. Hyder F, Kida I, Behar KL, Kennan RP, Maciejewski PK, Rothman DL. Quantitative functional imaging of the brain: towards mapping neuronal activity by BOLD fMRI. *NMR Biomed.* 2001; **14**(7–8): 413–431.
16. Thomas DL, Lythgoe MF, Calamante F, Gadian DG, Ordidge RJ. Simultaneous noninvasive measurement of CBF and CBV using double-echo FAIR (DEFAIR). *Magn. Reson. Med.* 2001; **45**(5): 853–863.
17. Yang Y, Frank JA, Hou L, Ye FQ, McLaughlin AC, Duyn JH. Multislice imaging of quantitative cerebral perfusion with pulsed arterial spin labeling. *Magn. Reson. Med.* 1998; **39**(5): 825–832.
18. Zhu XH, Kim SG, Andersen P, Ogawa S, Ugurbil K, Chen W. Simultaneous oxygenation and perfusion imaging study of functional activity in primary visual cortex at different visual stimulation frequency: quantitative correlation between BOLD and CBF changes. *Magn. Reson. Med.* 1998; **40**(5): 703–711.
19. Silva AC, Lee SP, Yang G, Iadecola C, Kim SG. Simultaneous blood oxygenation level-dependent and cerebral blood flow functional magnetic resonance imaging during forepaw stimulation in the rat. *J. Cereb. Blood Flow Metab.* 1999; **19**(8): 871–879.
20. Kruger G, Kastrup A, Takahashi A, Glover GH. Simultaneous monitoring of dynamic changes in cerebral blood flow and oxygenation during sustained activation of the human visual cortex. *Neuroreport* 1999; **29**;10(14): 2939–2943.
21. Reese T, Porszasz R, Baumann D, Bochelen D, Boumezbeur F, McAllister KH, Sauter A, Bjelke B, Rudin M. Cytoprotection does not preserve brain functionality in rats during the acute post-stroke phase despite evidence of non-infarction provided by MRI. *NMR Biomed.* 2000; **13**(6): 361–370.
22. Schwazbauer C. Simultaneous detection of changes in perfusion and BOLD contrast. *NMR Biomed.* 2000; **13**(1): 37–42.
23. Yongbi MN, Fera F, Mattay VS, Frank JA, Duyn JH. Simultaneous BOLD/perfusion measurement using dual-echo FAIR and UNFAIR: sequence comparison at 1.5T and 3.0T. *Magn. Reson. Imag.* 2001; **19**(9): 1159–1165.
24. Lai S, Wang J, Jahng GH. FAIR exempting separate T (1) measurement (FAIREST): a novel technique for online quantitative perfusion imaging and multi-contrast fMRI. *NMR Biomed.* 2001; **14**(7–8): 507–516.
25. Schutle AC, Speck O, Oesterle C, Hennig J. Separation and quantification of perfusion and BOLD effects by simultaneous acquisition of functional $I(0)$- and $T_2(*)$-parameter maps. *Magn. Reson. Med.* 2001; **45**(5): 811–816.
26. Miller KL, Luh WM, Liu TT, Martinez A, Obata T, Wong EC, Frank LR, Buxton RB. Nonlinear temporal dynamics of the cerebral blood flow response. *Hum. Brain Mapp.* 2001; **13**(1): 1–12.
27. Luh WM, Wong EC, Bandettini PA, Ward BD, Hyde JS. Comparison of simultaneously measured perfusion and BOLD signal increases during brain activation with T1-based tissue identification. *Magn. Reson. Med.* 2000; **44**: 137–143.
28. Song AW, Popp CA. fMRI using ADC contrast. *Proc. ISMRM* 1998; **6**: 1438.
29. Darquie A, Clark CA, van de Moortele PF, Le Bihan D. Comparison of BOLD and IVIM event-related fMRI. *Proc. ISMRM*, 1999; p. 447.
30. Song AW, Woldorff M, Gangstead S, Mangun GR, McCarthy G. Enhanced spatial localization of neuronal activation using simultaneous apparent-diffusion-coefficient and blood-oxygenation functional MRI. *NeuroImage* 2002; **17**: 742–750.
31. Le Bihan D, Breton E, Lallemand D, Grenier P, Cabanis E, Laval-Jeantet M. MR imaging of intravoxel incoherent motions: application to diffusion and perfusion in neurologic disorders. *Radiology* 1986; **161**: 401–407.
32. Le Bihan D, Turner R. The capillary network: a link between IVIM and classical perfusion. *Magn. Reson. Med.* 1992; **27**: 171–178.
33. Gangstead SL, Song AW. On the timing characteristics of apparent-diffusion-coefficient contrast fMRI. *Magn. Reson. Med.* 2002; **48**: 385–388.

34. Baramidze D, Mchedlishvili G, Gordeladze Z, Levkovitch Y. Cerebral microcirculation: heterogeneity of pial arterial network controlling microcirculation of cerebral cortex. *Int. J. Microcircul. Clin. Exp.* 1992; **11**: 143–155.
35. Ngai AC, Meno JR, Winn HR. Simultaneous measurement of pial arteriolar diameter and laser-doppler flow during somatosensory stimulation. *J. Cereb. Blood Flow Metab.* 1995; **15**: 124–127.
36. Malonek D, Dirnagl U, Lindauer U, Yamada K, Kanno I, Grinvald A. Vascular imprints of neuronal activity: relationships between the dynamics of cortical blood flow, oxygenation, and volume changes following sensory stimulation. *Proc. Natl Acad. Sci. USA* 1997; **94**: 14826–14831.
37. Darquie A, Poline JB, Poupon C, Saint-Jalmes H, Le Bihan D. Transient decrease in water diffusion observed in human occipital cortex during visual stimulation. *Proc. Natl Acad. Sci. USA* 2001; **98**: 9391–9395.
38. Wong EC, Cox RW, Song AW. Optimized isotropic diffusion weighting. *Magn. Reson. Med.* 1995; **34**: 139–143.
39. Zhong J, Kennan RP, Fulbright RK, Gore JC. Quantification of intravascular and extravascular contributions to BOLD effects induced by alteration in oxygenation or intravascular contrast agents. *Magn. Reson. Med.* 1998; **40**: 526–36.
40. Does MD, Zhong J, Gore JC. *In vivo* measurement of ADC change due to intravascular susceptibility variation. *Magn. Reson. Med.* 1999; **41**: 236–40.

